


RESEARCH

Open Access



# Establishment of porcine embryonic stem cells in simplified serum free media and feeder free expansion

Hyerin Choi<sup>1,2</sup>, Dongjin Oh<sup>1,2</sup>, Mirae Kim<sup>1,2</sup>, Ali Jawad<sup>1,2</sup>, Haomiao Zheng<sup>1,2</sup>, Lian Cai<sup>1</sup>, Joohyeong Lee<sup>5</sup>, Eunhye Kim<sup>6</sup>, Gabsang Lee<sup>7</sup>, Hyewon Jang<sup>8</sup>, Changjong Moon<sup>8</sup> and Sang-Hwan Hyun<sup>1,2,3,4\*</sup> 

## Abstract

**Background** The establishment of stable porcine embryonic stem cells (pESCs) can contribute to basic and biomedical research, including comparative developmental biology, as well as assessing the safety of stem cell-based therapies. Despite these advantages, most pESCs obtained from in vitro blastocysts require complex media and feeder layers, making routine use, genetic modification, and differentiation into specific cell types difficult. We aimed to establish pESCs with a single cell-passage ability, high proliferative potency, and stable in long-term culture from in vitro-derived blastocysts using a simplified serum-free medium.

**Methods** We evaluated the establishment efficiency of pESCs from in vitro blastocysts using various basal media (DMEM/F10 (1:1), DMEM/F12, and a-MEM) and factors (FGF2, IWR-1, CHIR99021, and WH-4-023). The pluripotency and self-renewal capacity of the established pESCs were analyzed under feeder or feeder-free conditions. Ultimately, we developed a simplified culture medium (FIW) composed of FGF2, IWR-1, and WH-4-023 under serum-free conditions.

**Results** The pESC-FIW lines were capable of single-cell passaging with short cell doubling times and expressed the pluripotency markers POU5F1, SOX2, and NANOG, as well as cell surface markers SSEA1, SSEA4, and TRA-1-60. pESC-FIW showed a stable proliferation rate and normal karyotype, even after 50 passages. Transcriptome analysis revealed that pESC-FIW were similar to reported pESC maintained in complex media and showed gastrulating epiblast cell characteristics. pESC-FIW were maintained for multiple passages under feeder-free conditions on fibronectin-coated plates using mTeSR™, a commercial medium used for feeder-free culture, exhibiting characteristics similar to those observed under feeder conditions.

**Conclusions** These results indicated that inhibition of WNT and SRC was sufficient to establish pESCs capable of single-cell passaging and feeder-free expansion under serum-free conditions. The easy maintenance of pESCs facilitates their application in gene editing technology for agriculture and biomedicine, as well as lineage commitment studies.

**Keywords** Embryonic stem cells, Pig, Pluripotency, Self-renewal, Serum-free media

\*Correspondence:  
Sang-Hwan Hyun  
shyun@cbsu.ac.kr

Full list of author information is available at the end of the article



© The Author(s) 2024. **Open Access** This article is licensed under a Creative Commons Attribution-NonCommercial-NoDerivatives 4.0 International License, which permits any non-commercial use, sharing, distribution and reproduction in any medium or format, as long as you give appropriate credit to the original author(s) and the source, provide a link to the Creative Commons licence, and indicate if you modified the licensed material. You do not have permission under this licence to share adapted material derived from this article or parts of it. The images or other third party material in this article are included in the article's Creative Commons licence, unless indicated otherwise in a credit line to the material. If material is not included in the article's Creative Commons licence and your intended use is not permitted by statutory regulation or exceeds the permitted use, you will need to obtain permission directly from the copyright holder. To view a copy of this licence, visit <http://creativecommons.org/licenses/by-nc-nd/4.0/>.

## Background

Stable livestock pluripotent stem cells (PSCs) are a promising resource for basic and biomedical research, including comparative developmental biology [1], as well as the genetic modification of animal hosts for xenotransplantation [2]. Particularly, mesenchymal stem cells, which are readily accessible, are increasingly utilized in clinical applications within the field of regenerative medicine [3, 4]. Compared to other species, stable pig PSCs are regarded as ideal models for informative applications in human developmental modeling because of their similarities in terms of embryo development [1], anatomy, and physiology [5–7].

Based on previously reported culture conditions of human and mouse PSCs, there have been many attempts to establish pig PSCs since the 1990s [8–16]. However, they remain unstable in long-term culture and lack defined pluripotency features. This may be due to insufficient analysis and understanding of the specific pluripotency mechanisms in different species.

In 2019, there were notable advances in pig PSCs: first, pig expanded potential stem cells (EPSCs) that had developmental potential for all embryonic and extraembryonic cell lineages, allowed genome editing, and were capable of differentiating into chimeric trilineage derivatives were reported [17]. Due to the lack of information on the molecular mechanisms of preimplantation embryonic development in the pigs at the time of the study, the culture conditions for pig EPSCs were determined through a combination of inhibitors required to maintain mouse and human PSCs. Meanwhile, Ramos-Ibeas et al. provided insights into pig pluripotency status and lineage delineation by conducting molecular characterization of the inner cell mass and trophectoderm of pig early blastocysts and the progressive separation of epiblasts and hypoblasts in late blastocysts at single cell resolution [18]. In addition, several pig embryonic stem cells (pESCs) established under defined culture conditions without the use of fetal serum have been reported [19–24]. Most recently, a culture medium was developed to establish a stable PSC line from pig embryonic day (E) 10 pregastrulation epiblasts (pgEpiSCs) based on a large-scale single-cell transcriptome analysis of pig embryos from E0 to E14 [24]. By combining chemical-induced inhibition of WNT-related signaling with growth factors from the FGF/ERK, JAK/STAT3, and Activin/Nodal pathways, pgEpiSCs maintained pluripotency transcriptome features similar to E10 epiblasts and were stable for over 240 passages. This advance in pig PSCs from 2019 could be a starting point for increasing their utilization and application in various research fields.

Despite these advances, there are still issues that need to be addressed. Recently developed culture conditions for EPSCs [17] and pgEpiSCs [24] are suitable for in

vivo-derived E5 blastocysts and E10 epiblasts, respectively. Although the quality of in vivo-derived embryos is generally higher than that of in vitro-derived ones, obtaining in vivo-derived embryos is limited by technical barriers and requires high costs. In addition, complex media containing more than five cocktails are required to maintain PSCs to minimize the use of serum [19, 21, 22]. The complexity cause batch-to-batch variation between laboratories and can lead to low utilization of PSCs. Therefore, we aimed to establish pESCs with single cell-passage ability, high proliferative potency, and stable in long-term culture from in vitro-derived blastocysts using a simplified serum-free medium. A pESC line that is easy to establish and maintain can provide a cell source with low experimental barriers and costs for genetic manipulation, induction of specific cell types, and further studies of cellular behavior.

## Methods

### Animals and samples

Pig ovaries were donated by a local slaughterhouse (Dong-A Food, Republic of Korea). E13.5 ICR mice and BALB/c nude mice were purchased from DBL (Seoul, Republic of Korea) and OrientBio (Seongnam, Republic of Korea), respectively. Euthanization was performed under cervical dislocation, and all efforts were made to minimize suffering.

### Oocyte collection and in vitro maturation (IVM)

About 100–120 porcine ovaries were obtained daily at a local slaughterhouse and transported to the laboratory within 3 h in 0.9% (w/v) NaCl saline at 37–39 °C. Porcine follicular fluid (pFF) containing cumulus-oocyte complexes (COCs) was aspirated from the antral follicles (3–6 mm) using a 10-mL disposable syringe with an 18-G needle and collected into a 15-mL centrifuge tube. After settling at 37 °C for 5 min, the supernatant was removed, and the precipitate was resuspended in HEPES-buffered Tyrode's medium containing 0.05% (w/v) polyvinyl alcohol (TLH-PVA) and 300–320 COCs were recovered using a stereomicroscope. Only COCs with three or more layers of compact cumulus cells and a homogenous cytoplasm were selected for IVM. The selected COCs were transferred to 500 µl of TCM199 (Gibco, Grand Island, NY, United States) supplemented with 0.6 mM cysteine, 0.91 mM sodium pyruvate, 10 ng/mL epidermal growth factor, 75 µg/mL kanamycin, 1 µg/mL insulin, and 1% (w/v) pFF. For maturation, the selected COCs were incubated for 42 h at 39 °C with 5% CO<sub>2</sub> and 95% air in a humidified chamber. During the first 22 h, the COCs were matured using hormones (10 IU/mL equine chorionic gonadotropin and 10 IU/mL hCG (Intervet, Boxmeer, Netherlands)). After 22 h of maturation with hormones, COCs were cultured in the absence of eCG

and hCG in the maturation medium for an additional 18–20 h.

#### Parthenogenetic activation (PA)

After 42 h of IVM, oocytes that included the first polar body were selected for PA. The collected oocytes were washed twice with 280 mM mannitol solution containing 0.01 mM CaCl<sub>2</sub> and 0.05 mM MgCl<sub>2</sub>. Then, the oocytes were loaded on the activation solution (260 mM mannitol solution supplemented with 0.001 mM CaCl<sub>2</sub> and 0.05 mM MgCl<sub>2</sub>) between the electrodes of the chamber. The chamber was connected to an electrical pulsing machine (LF101; Nepa Gene, Chiba, Japan), and the oocytes loaded in the electrodes were activated with two pulses of 120 V/mm DC for 60 μs. The activated oocytes were transferred into an IVC medium (porcine zygote medium 3) containing 5 μg/mL cytochalasin B and incubated in a 39 °C humidified atmosphere of 5% CO<sub>2</sub> and 5% O<sub>2</sub> for 4 h. After that, the PA embryos were washed twice with IVC medium, and 10–12 embryos were cultured in 25-μL droplets of fresh IVC medium covered with mineral oil. The medium was changed every two days.

#### In vitro fertilization (IVF) of porcine oocytes

To perform IVF, MII oocytes were selected and washed twice with modified Tris-buffered medium (mTBM) [25], transferred to 40 μL droplets (15 oocytes/drop) of mTBM, and incubated in a 39 °C humidified atmosphere of 5% CO<sub>2</sub> until fertilization. Fresh boar liquid semen was delivered twice a week by a local artificial insemination center (Xperm-V; Darby Genetics, Inc., Anseong, South Korea) and stored at 17 °C until use. The semen was washed twice with Dulbecco's phosphate-buffered saline (DPBS) containing 0.1% BSA by centrifugation at 2,000 rpm for 2 min. After washing, the sperm pellets were resuspended in pre-warmed mTBM. The sperm motility was assessed under a stereomicroscope (Olympus), and only >70% of motile sperm were used for IVF. The sperm concentration was determined using a hemocytometer, and the sperm was diluted with mTBM. The MII oocytes were co-incubated with the sperm at a final concentration of 5 × 10<sup>5</sup> sperm/mL for 20 min at 39 °C in a 5% CO<sub>2</sub> humidified incubator. Afterward, loosely attached sperm were removed from the zona pellucida (ZP) by gentle pipetting. The oocytes were washed twice and incubated in mTBM without sperm for 5–6 h at 39 °C in a 5% CO<sub>2</sub> humidified incubator. The presumptive IVF zygotes were washed and cultured in 25-μL droplets of fresh IVC medium covered with mineral oil in a humidified incubator with 5% CO<sub>2</sub> and 5% O<sub>2</sub>. The medium was changed every two days. On day 4, 10% fetal bovine serum (FBS) was added to the IVC droplets, which contain embryos.

#### Culture of porcine induced pluripotent stem cells (iPSC)

The piPSC-LIF cell lines utilized in this study were generously provided by Professor Jongpil Kim (Dongguk University, Republic of Korea). Cell lines were generated by the lentiviral transfection of porcine embryonic fibroblasts (PEFs) with four doxycycline-inducible human factors obtained from Addgene: FUW-tetO-hOct4, FUW-tetO-hSox2, FUW-tetO-hKlf4, FUW-tetO-hcMyc, and FUW-M2rtTA. These cells were cultured in a mixture of DMEM and F10 (in a 50:50 ratio), supplemented with 15% FBS, 1 × Glutamax, 1 × β-mercaptoethanol, 1 × MEM non-essential amino acids, 1 × antibiotic/antimitotic solution, 1000 units/mL LIF (LIF2010, Millipore), and 2 μg/mL doxycycline (D9891, Sigma). The piPSC-FGF lines [26] were provided by Professor Gabsang Lee (Johns Hopkins University, USA). The medium contained DMEM/F12, 20% KSR, 1 × Glutamax, 1 × MEM non-essential amino acids, 1 × β-mercaptoethanol, and 10 ng/mL FGF2. Two piPSC lines were cultured in 4-well dishes on mitotically inactivated MEF feeder cells and maintained at a temperature of 38.5 °C in a 5% CO<sub>2</sub> air atmosphere. The culture medium was changed daily, and the cells were passaged every 3 days using 0.04% trypsin solution.

#### Test of basal media and signaling molecules for deriving pESC

To identify simplified culture conditions for establishing pig ESCs, we obtained day 6 blastocysts after performing PA or IVF and seeded unhatched blastocysts on MEF feeder cells. To compare the efficiency of the pESCs establishment, the seeded blastocysts were cultured with DMEM/F10 (1:1), DMEM/F12, and α-MEM medium. We also tested small-molecule combinations of (1) FGF2 (F), (2) FGF2+IWR-1 (FI), and (3) FGF2+IWR-1+CHIR (FIC). The basal medium was composed of 10% KSR (Gibco, Gaithersburg, MD, USA), 1X non-essential amino acids, 0.05 mM β-mercaptoethanol, and 1% antibiotic-antimycotic. The tested small molecules were 10 ng/mL recombinant human fibroblast growth factor-basic (FGF2; Peprotech, 100-18B), 1.5 μM IWR-1 (Sigma-Aldrich, I0161), and 0.5 μM CHIR99021 (CH; Selleckchem, S1263). At 10 days after blastocyst seeding, primary colonies of porcine ESCs were observed and then fixed with 4% (w/v) paraformaldehyde. Cultures were performed under humidified conditions in an atmosphere containing 5% CO<sub>2</sub> at 37 °C.

#### Maintenance and culture of pESC-FIW

For routine maintenance, pESC were cultured on MEF feeder cells in FIW medium under 5% CO<sub>2</sub> at 37 °C with daily medium exchange. The basal medium of the FIW was composed of DMEM/F12, 10% KSR, 1 × non-essential amino acids, 0.05 mM β-mercaptoethanol, and

1% antibiotic-antimycotic. To prepare the FIW medium, 10 ng/mL FGF2, 1.5  $\mu$ M IWR-1, and 0.3  $\mu$ M WH-4-023 (Selleckchem, S7565) were added to the basal medium. The concentrations of each factor were determined by referring to information used in culturing pig PSCs [17, 20, 24]. The FIW medium can be stored for a week at 4 °C and used after leaving it at room temperature for 5 min. pESC-FIW cells were dissociated using TrypLE™ Express Enzyme (Gibco, 12,605,010) and passaged every 3–4 days at a ratio of 1:5 to 1:10 in the presence of 10  $\mu$ M ROCKi, which was added 24 h after passage.

#### Spontaneous differentiation of pESC-FIW in vitro using the embryoid body method

Cultured pESCs were dissociated into single cells using TrypLE Express and cultured on 35-mm low-attachment plates in DMEM (Gibco, 11960-044) supplemented with 10% (v/v) FBS (Gibco, 16,000,044) and 10  $\mu$ M ROCKi (24 h only) without other small molecules for 7 days. After suspension culture, the aggregated cells were harvested, plated on 0.1% (w/v) gelatin-coated plates, and cultured for 10 days in the same medium. The resulting differentiated cells were fixed in 4% (w/v) paraformaldehyde for immunofluorescence.

#### Directional-induced differentiation

We attempted to directionally induce the differentiation of pESC-FIW cells using a previously described conditioned media composition [24]. For neural induction, the F12-FIW culture medium was replaced with neural induction medium I (2.5  $\mu$ M IWR-1, 5  $\mu$ M SB431542, and 10 ng/mL FGF2 in F12 media) on day 2 after plating pESCs on Matrigel-coated plates. After culturing for 3 more days, the pESCs were transferred to a new Matrigel-coated plate, and the medium was changed to neural induction medium II (4  $\mu$ M RA, 10 ng/mL FGF2, and 20 ng/mL Noggin in F12 media). Immunostaining was performed 2 days later. For endoderm induction, pESCs, which had been cultured for 2 days on Matrigel-coated plates, were exposed to the F12 medium containing 10 ng/mL BMP4, 5  $\mu$ M SB431542, and 10 ng/mL FGF2 for 3 days, followed by immunostaining. For mesoderm induction, the F12-FIW culture medium was changed to mesoderm induction medium I (10 ng/mL BMP4, 50 ng/mL Activin A 20 ng/mL FGF2 in F12 medium) 2 days after plating pESCs on Matrigel-coated plates. After culturing for 2 more days, the pESCs were transferred to a new Matrigel-coated plate, medium I was changed to mesoderm induction medium II (3  $\mu$ M IWR-1-endo, 5  $\mu$ M CHIR99021, and 20 ng/mL FGF2 in F12 media), and immunostaining was performed 2 days later.

#### Teratoma formation

For the teratoma formation assay, dissociated pESC-FIW were collected by centrifugation at 3000 rpm for 2 min and injected at a concentration of  $1 \times 10^7$  cells into the posterior flank and  $2.5 \times 10^6$  cells into the gastrocnemius muscle of 6–8-week old male BALB/c nude mice. A total of 2 mice were used for the injections. Teratomas were seen after 4 weeks of growth and performed sampling at 6 weeks. Samples were collected and fixed with 10% neutral buffered formalin for overnight at 4 °C. After fixation, the samples were trimmed and washed for 2 h with running tap water, dehydrated in a succession of ethanol concentrations (70%, 80%, 90%, 95%, and 100% for 1 h each), cleaned in xylene, embedded in paraffin. Samples were sliced to 3  $\mu$ m thickness, deparaffinized in xylene and rehydrated with decreasing concentration of ethanol. Following deparaffinization, the sections were utilized for hematoxylin and eosin staining, and observed under MoticEasyScan One.

#### Cell growth curve and population doubling time

Pig PSCs were cultured in 4-well plates. Triplicate samples of cells were seeded at a density of  $0.5 \times 10^5$  cells/well. The cells were counted every 24 h. For each time point, the cells were detached and counted using a hemocytometer. The counts were averaged over three replicates. The cell doubling time (DT) was calculated as follows:  $DT = 24 \times [\lg_2 / (\lg N_t - \lg N_0)]$ , where 24 is the cell culture time (h),  $N_t$  is the number of cells cultured for 48 h, and  $N_0$  is the number of cells recorded at 24 h.

#### Analysis of single-cell clonal efficiency

Cells were dissociated using TrypLE™ Express Enzyme (Gibco, 12605010), counted using a hemocytometer, and plated onto pre-seeded 4-well plate feeders at a density of 1,000 cells per well in triplicate under FIW culture conditions. Colonies were counted 6 days later using AP staining, and the colony formation efficiency was evaluated as the percentage of colonies per number of seeded cells.

#### Karyotype analyses

Karyotyping of cells using standard G-banding chromosomes and cytogenetic analysis were performed at the Korea Research of Animal Chromosomes ([www.krach.co.kr](http://www.krach.co.kr), Korea).

#### Alkaline phosphatase (AP) staining

AP staining of pESC-FIW was performed using NBT/BCIP stock solution (Roche, Basel, Switzerland, 11,681,451,001). A total of 20  $\mu$ l of stock solution was dissolved in 1 mL 0.1 M Tris-HCl, pH 9.5, and added to the cells fixed with 4% paraformaldehyde.

### Immunofluorescence analysis

Cells were washed with DPBS (Welgene, LB 001–02), fixed with 4% paraformaldehyde at room temperature for 10 min, washed with DPBS three times, permeabilized in 0.5% Triton X-100 for 10 min, and blocked with 3% BSA for 30 min. The cells were incubated with primary antibodies diluted with 3% BSA at 4 °C overnight. The cells were then washed thrice with DPBS for 5 min. Secondary antibodies were diluted and incubated with wash buffer at room temperature for 1 h, washed with wash buffer three times for 5 min each, and stained with Hoechst (Invitrogen, H3570) for 10 min. The antibodies used are listed in Supplementary Information Table S1.

### RT-qPCR

All samples were washed twice in Dulbecco's PBS and stored at –80 °C until mRNA extraction. Total RNA was extracted using the TRIzol reagent (TaKaRa Bio, Inc., Otsu, Japan), and complementary DNA (cDNA) was synthesized using a reverse transcription master mix (Elpis Bio, Inc., Chungcheongnam-do, Daejeon, Republic of Korea) according to the manufacturer's instructions. For qRT-PCR, the synthesized cDNA, 2× SYBR Premix Ex Taq (TaKaRa Bio, Inc.), and 10 pmol of specific primers (Macrogen) were added to prepare the PCR mixture. All primer sequences used in this study are listed in Table S2. qRT-PCR was performed using a CFX96 Touch Real-Time PCR Detection System (Bio-Rad, Hercules, CA, United States). The reactions were performed as follows: 40 cycles of denaturation at 95 °C for 30 s, annealing at 58 °C for 15 s, and extension at 72 °C for 30 s. Relative quantification was performed using threshold cycle (Ct)-based methodologies at a constant fluorescence intensity. The relative mRNA expression (R) was calculated using the equation  $R = 2^{-(Ct_{sample} - Ct_{control})}$ . The R-values obtained for each gene were normalized to *RN18S*.

### Transcriptome analysis

Total RNA was extracted from the three pESC-FIW (PA\_1\_pESC\_FIW; PA\_3\_pESC\_FIW; IVF\_1\_pESC\_FIW) for construction cDNA libraries. RNA extraction, cDNA library preparation, and RNA-seq analysis were performed using TheraGen ETEX ([www.theragenetex.com](http://www.theragenetex.com); Korea). Libraries were prepared for 151 bp paired-end sequencing using the TruSeq stranded mRNA Sample Preparation Kit (Illumina, CA, USA). mRNA molecules were purified and fragmented from 1 µg of total RNA using oligo (dT) magnetic beads. The fragmented mRNAs were synthesized as single-stranded cDNAs using random hexamer priming. By using this as a template for second-strand synthesis, double-stranded cDNA was prepared. After sequential end repair, A-tailing, and adapter ligation, cDNA libraries were amplified by PCR. The quality of cDNA libraries was evaluated using an

Agilent 2100 BioAnalyzer (Agilent, CA, USA; Table S3). They were quantified using a KAPA library quantification kit (Kapa Biosystems, MA, USA) according to the manufacturer's library quantification protocol. Following cluster amplification of the denatured templates, paired-end sequencing (2×151 bp) using an Illumina NovaSeq6000 (Illumina, CA, USA) was performed.

### Transcriptome data analysis

The adapter sequences and the ends of the reads less than Phred quality score 20 were trimmed and simultaneously the reads shorter than 50 bp were removed by using cutadapt v.2.8 [27]. Filtered reads were mapped to the reference genome related to the species using the aligner STAR v.2.7.1a [28] following ENCODE standard options (refer to "Alignment" of "Help" section in the html report) with "-quantMode TranscriptomeSAM" option for estimation of transcriptome expression level. Gene expression estimation was performed by RSEM v.1.3.1 [29] considering the direction of the reads which are corresponding to the library protocol using option "--strandedness". To improve the accuracy of the measurement, "--estimate-rspd" option was applied. All other options were set to default values. To normalize sequencing depth among samples, FPKM and TPM values were calculated.

### Adaptation of feeder-cultured pESC to feeder-free conditions

To screen the extracellular matrix that could functionally replace Matrigel, the selected matrix proteins were coated according to the manufacturer's suggestions. The coated plates were used immediately or sealed and stored at 4 °C for up to two weeks. All experiments were performed in at least three replicates for each matrix protein. pESCs were harvested at 1.5, 24, and 72 h after seeding, and the cell number was counted using a hemocytometer. The matrix proteins tested were Matrigel (Corning, 354,277), Fibronectin (Thermo Fisher Scientific, 33,010,018), Laminin-521 (Gibco, A29248), and VTN-N (Gibco, A14700). The pESCs cultured on the feeder layer were dissociated using TrypLE™ Express Enzyme and seeded on a plate coated with each of the four different extracellular matrices (Matrigel, Fibronectin, Laminin 521, and VTN-N). The medium was replaced with a commercial mTeSR culture medium. FF-pESCs were passaged every 3–4 days at a ratio of 1:3 to 1:5.

### Statistical analysis

Statistical analyses were performed using the Prism software (version 8.0; GraphPad Software, San Diego, CA, USA). Results are expressed as mean ± standard error of the mean (SEM). Experiments were repeated at least three times unless a different number of repeats was

specified in the legend. Statistical analyses were performed using an unpaired two-tailed Student's *t*-test or ANOVA.  $p < 0.05$  was considered statistically significant. The statistical methods, *p*-values, and sample numbers are indicated in the figure legends.

The work has been reported in line with the ARRIVE guidelines 2.0.

## Results

### Optimization of culture conditions for establishing porcine embryonic stem cells

To develop a simplified media for the establishment and maintenance of pESCs, we used a culture medium consisting of a minimal combination of small molecules in knockout serum replacement medium. Blastocysts obtained in vitro on day 6 were seeded on the feeder cell layer with DMEM/F10 (1:1), DMEM/F12, and  $\alpha$ -MEM medium to compare the efficiency of the pESCs establishment according to the type of the basal medium and small molecules. Based on the recently revealed pig pluripotency network information [18, 24], the ERK/MEK pathway factor FGF2 and WNT pathway-related inhibitors IWR-1 (WNT inhibitor) and CHIR (WNT activator) were applied. The small-molecule conditions were (1) FGF2 (F), (2) FGF2+IWR-1 (FI), and (3) FGF2+IWR-1+CHIR (FIC). Colony formation was observed only in the DMEM/F10 and DMEM/F12 cells (Table 1; Fig. 1A). Outgrowths from both media under FI and FIC conditions showed typical expression of SOX2, which is an ICM marker of early blastocyst in pigs [30] (Fig. 1B). Unexpectedly, the FIC condition showed a tendency to direct pESCs to a neural fate (data not shown) from the early passage. Therefore, pESCs obtained under the FI conditions in DMEM/F12 (pESC-FI), the most defined and simplified culture medium, were ultimately maintained for further experiments. However, pESC-FI showed a low cell proliferation rate and

single-cell clonal efficiency compared to other pig PSC lines (piPSC-FGF and piPSC-LIF) (Fig. 1C-E). This indicates that the applied culture condition cannot support the self-renewal of pESC-FI. We attempted to enhance the self-renewal capacity of pESCs by adding the SRC inhibitor WH-4-023, which blocks epithelial-mesenchymal transition (EMT) and maintains self-renewal of naive human stem cells and pgEpiSCs [24, 31]. As a result, a new pESCs line (pESC-FIW) with a short cell doubling time and improved single-cell clonal efficiency was established. Furthermore, WH-4-023 contributed to the upregulation of proliferation-related genes and downregulation of EMT-related genes (Fig. 1F and G). We established a total of six cell lines from PA and IVF embryos (Fig. 1H). These results indicate that the addition of FGF2 and Wnt and SRC pathway inhibitors is sufficient to maintain pESCs with high proliferation potency and single-cell clonal efficiency.

### Characterization of an established pESC-FIW

We characterized the established pESC-FIW. As a result of immunostaining, pESC-FIW showed homogenous expression of the pluripotency factors POU5F1, NANOG, and SOX2 (Fig. 2A) and cytoplasmic distribution of the cell surface markers SSEA-1, SSEA-4, and TRA-1-60, except for TRA-1-81 (Fig. 2B). To confirm whether a stable long-term culture of pESCs is possible, their characteristics were compared by dividing them into early (p30 or less) and late passages (p50 or more). The morphology (Fig. 2C) and alkaline phosphatase (AP) activity (Fig. 2D) of the two passages were similar, and both showed a normal karyotype (Fig. 2E). A similar number of cells was observed in the cell proliferation curve for 96 h (Fig. 2F), and the doubling time was approximately 11 h, indicating active proliferation (Fig. 2G). Additionally, we obtained approximately 15% of single-cell clonal efficiency (Fig. 2H). The findings

**Table 1** An efficiency comparison of the pESC establishment in various serum-free media

Type of medium	Cytokines	No. of blastocysts seeded*	No. (%) of		Colonies maintained over two passages
			Parthenogenetic activation blastocysts attached to feeder cells	Colonies formed from blastocysts	
DMEM/F10	F	40	13 (29.4 ± 11.8)	2 (3.9 ± 3.9)	ND <sup>a</sup>
	FI	40	13 (34.8 ± 7.9)	4 (9.2 ± 5.1)	2
	FIC	39	15 (37.9 ± 10.6)	3 (6.7 ± 3.5)	2
DMEM/F12	F	35	11 (30.8 ± 14.5)	7 (20.0 ± 2.6)	ND
	FI	35	10 (28.0 ± 9.8)	3 (8.3 ± 8.3)	2
	FIC	35	15 (42.4 ± 9.0)	3 (8.3 ± 4.8)	3
$\alpha$ -MEM	F	31	15 (51.6 ± 17.5)	ND	ND
	FI	31	14 (46.8 ± 10.9)	ND	ND
	FIC	31	12 (37.3 ± 6.5)	ND	ND

\* 3 times replicated

<sup>a</sup> Not detected; colonies cultured under these conditions were not maintained after seeding or subculturing

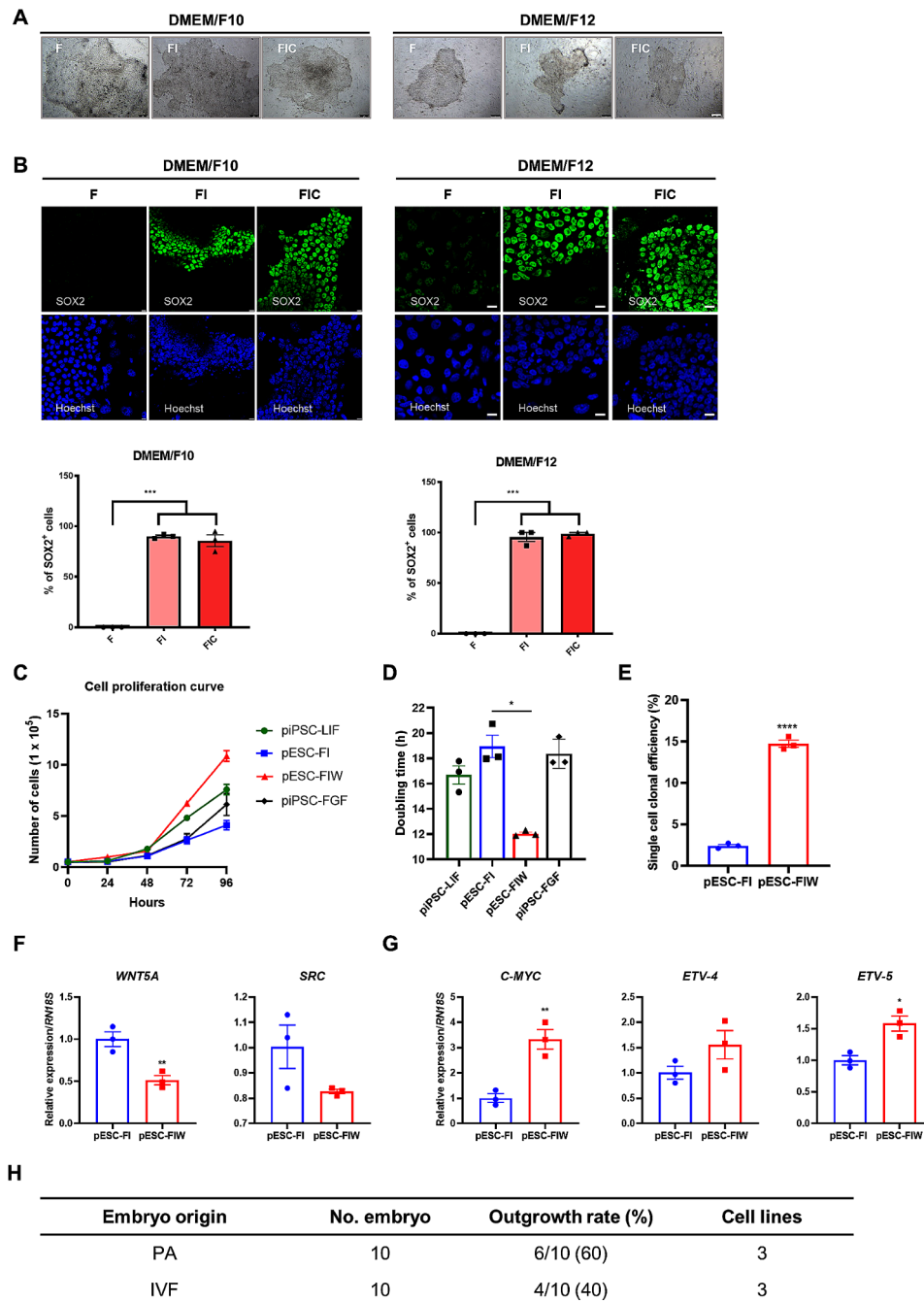


**Fig. 1** Optimizing culture conditions for pig embryonic stem cells (pESCs). **A** Bright-field images of colonies formed in different media. Images represent day 10 or day 12 after the seeding of blastocysts on the feeder layer. Scale bar, 250  $\mu$ m. **B** Representative images and quantitative analysis of SOX2 expression in pESCs-like colonies cultured with various media. Hoechst was used to stain nuclei. Scale bar, 20  $\mu$ m. **C** Cell proliferation curve of pESC-FI, pESC-FIW, piPSC-LIF, and piPSC-FGF. The initial cell count was  $0.5 \times 10^5$ . **D** Population doubling time. **E** Single cell clonal efficiency. **F, G** Quantification of mRNA expression of EMT (**F**) and proliferation-associated genes (**G**) by qRT-PCR. Cell line PA\_3\_pESC\_FIW were used. **H** The information of the established cell lines from PA and IVF embryos. For all graphs, the value represents the mean  $\pm$  SEM. Asterisks indicate statistical significance (\* $p < 0.05$ , \*\* $p < 0.01$ , \*\*\* $p < 0.001$ , \*\*\*\* $p < 0.0001$ )

indicate that pESCs with short doubling time and stable long-term culture ability can be established using the newly developed simplified serum-free medium.

We added the canonical WNT inhibitor IWR-1, and the SRC inhibitor WH-4-023 along with FGF2 to the

culture medium. We removed each of the factors from the culture medium to investigate their effects on pESC-FIW. The absence of FGF2 drastically reduced cell survival, and the cells could not be maintained for more than two passages (data not shown). When each inhibitor was

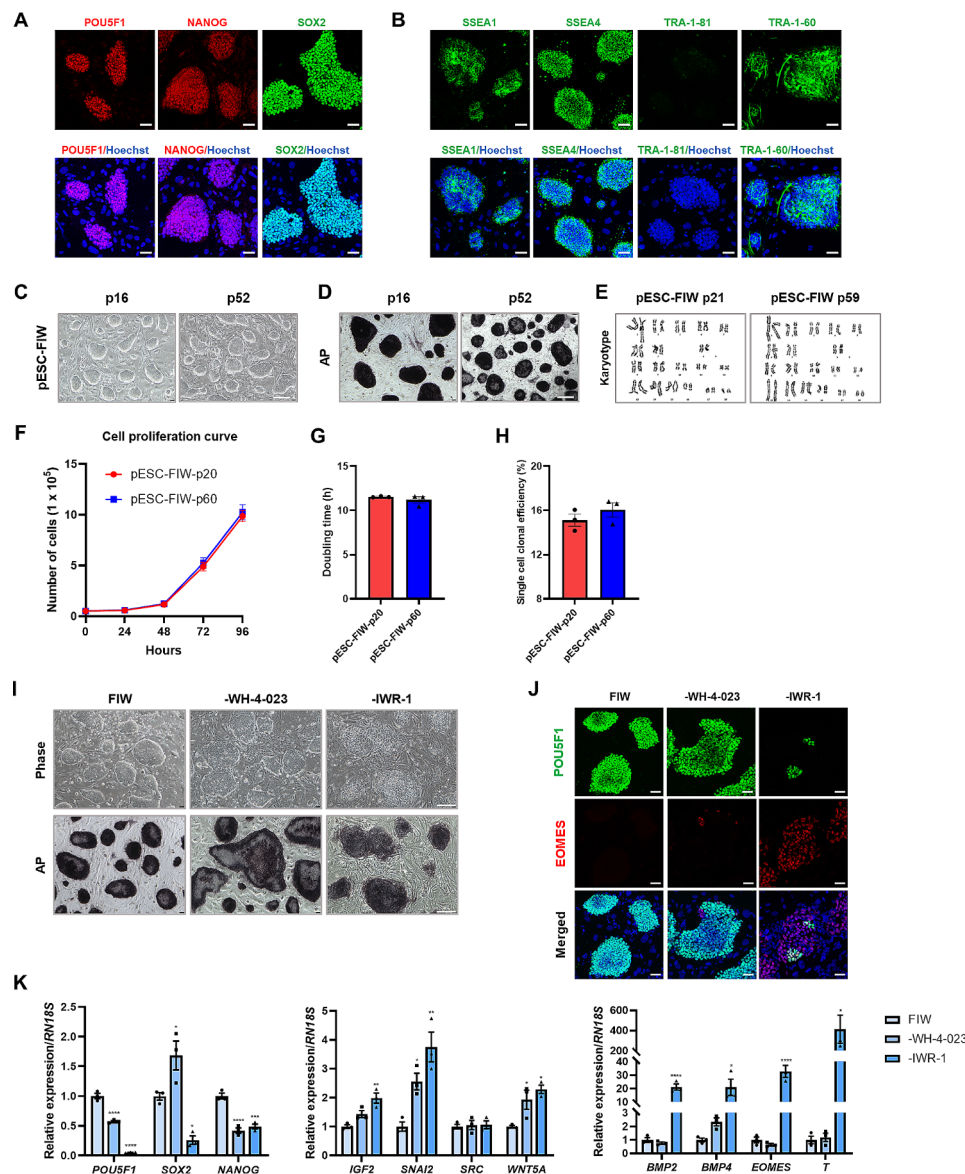


**Fig. 2** Characterization of established pESC-FIW. **A** Immunostaining of the pluripotency markers POU5F1, NANOG, and SOX2 in pESC-FIW. Hoechst was used to stain nuclei. Scale bar, 50  $\mu$ m. **B** Immunostaining of pluripotency surface markers SSEA1, SSEA4, TRA-1-81, and TRA-1-60 in the pESC-FIW colonies. Hoechst for staining of nuclei. Scale bar, 50  $\mu$ m. **C** Morphology of low- and high-passage pESC-FIW colonies. Scale bars, 200  $\mu$ m. **D** Alkaline phosphatase (AP) staining assay for low and high passage numbers of pESC-FIW colonies. Scale bars, 200  $\mu$ m. **E** Karyotype of low- and high-passage pESC-FIW colonies. **F** Cell proliferation curve of low- and high-passage pESC-FIW colonies. The initial cell count was  $0.5 \times 10^5$ . **G** Population doubling time of pESC-FIW. **H** Single-cell cloning efficiency of pESC-FIW. **I** Comparison of morphology and AP staining in pESC-FIW colonies cultured without WH-4-023 or IWR-1. Scale bar, 200  $\mu$ m. **J** Immunostaining for the pluripotency marker POU5F1 and mesoderm/endoderm progenitor marker EOMES. The nucleus is indicated by Hoechst. Scale bar, 50  $\mu$ m. **K** Quantification of mRNA expression of representative pluripotent marker genes involved in core pluripotency (left), EMT (middle), and gastrulation (right) by qRT-PCR. For all graphs, the value represents the mean  $\pm$  SEM. Asterisks indicate statistical significance (\*  $p < 0.05$ , \*\*  $p < 0.01$ , \*\*\*  $p < 0.001$ , \*\*\*\*  $p < 0.0001$ ). Cell line PA\_3\_pESC\_FIW were used.

removed, the dome-shaped cell morphology disappeared, and the cells showed a flat shape (Fig. 2I). The immunostaining results showed that the absence of WH-4-023 caused the appearance of the gastrulation marker EOMES in some cells, and the removal of IWR-1 turned off the expression of POU5F1 and increased EOMES expression in most cells (Fig. 2J). In the comparative analysis of gene expression, the core pluripotency gene

*POU5F1* was significantly decreased when WH-4-023 was removed (Fig. 2K, left), and the EMT-related genes *SNAI2* and *WNT5A* were significantly increased (Fig. 2K, middle). In the group in which IWR-1 was removed, all three core pluripotency genes showed a significant decrease (Fig. 2K, left), and both EMT- (Fig. 2K, middle) and gastrulation-related genes (Fig. 2K, right) showed a significant increase. It seems that inhibition of the Wnt



pathway plays a more pivotal role in preventing spontaneous differentiation of pESCs through processes, such as EMT and gastrulation, than inhibition of the SRC pathway.

The differentiation ability was confirmed *in vitro* to evaluate the pluripotency of pESC-FIW. First, we performed an embryoid body (EB) formation assay (Fig. 3A). Cells outgrowing from EBs on day 7 expressed ectodermal (Tubulin- $\beta$ III), mesodermal (T), and endodermal (CK17) markers. This indicated that pESC-FIW could spontaneously differentiate into the three germ layers when FGF2, IWR-1, and WH-4-023 were removed from

the medium (Fig. 3B). Next, we conducted a directional-induced differentiation assay and showed that pESC-FIW could differentiate into the three expected germ layers when exposed to neural, endoderm, and mesoderm-conditioned media (Fig. 3C). Finally, teratoma formation assays were conducted and confirmed that pESC-FIW developed into the expected tissues representative of three germ layers *in vivo* (Fig. 3D). Taking together, the differentiation ability of pESC-FIW was confirmed both *in vitro* and *in vivo*.

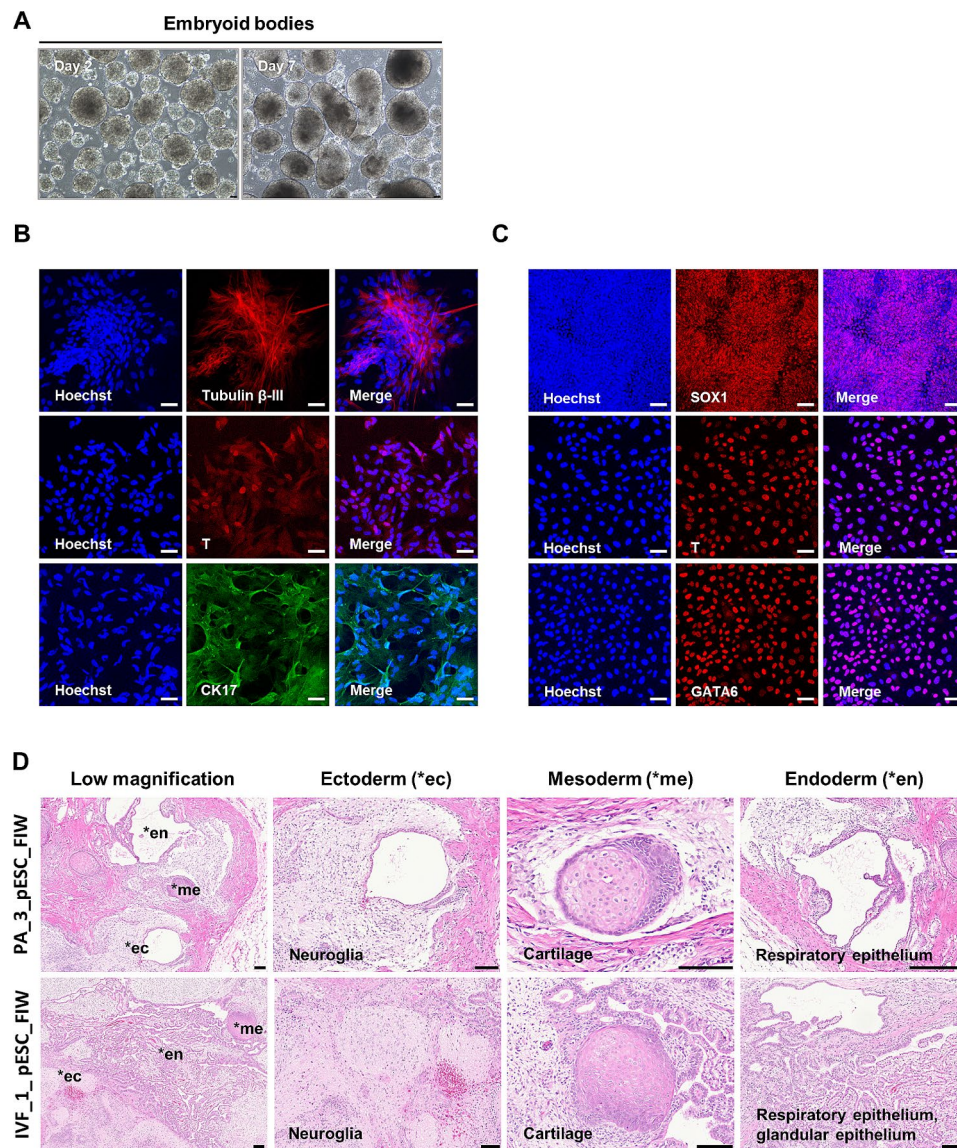


**Fig. 3** Evaluation of multilineage commitment of pESC-FIW. **A** Days 2 and 7 of embryoid bodies (EBs) derived from established pESC-FIW. Scale bar, 20  $\mu$ m. **B** The expression of the differentiation markers Tubulin  $\beta$ -III (ectoderm), T (mesoderm), and CK17 (endoderm) from EBs-derived cells. **C** Immunostaining of pESC-FIW after directional induced differentiation. SOX1 is a neural ectoderm marker, T is a mesoderm marker, GATA6 is an endoderm marker. Hoechst was used for nucleus staining. Scale bar, 50  $\mu$ m. Cell line PA\_3\_pESC\_FIW were used. **D** Teratoma formation from injected pESC-FIW. Scale bar, 100  $\mu$ m.

### Comparison of pluripotency features in established pESC-FIW with other pluripotent stem cells (PSCs)

Using two types of piPSCs (piPSC-LIF and piPSC-FGF) as relevant controls, we attempted to identify the pluripotent state of the established pESC-FIW. In the immunofluorescence data, pESC-FIW showed negative expression of the naïve marker *KLF4* and primed

marker *T* while showing homogenous expression of the formative marker *OTX2* (Fig. 4A). Next, a comparative analysis of representative pluripotency marker genes was conducted. Analysis of transcript levels of specific genes associated with the three pluripotent states showed the absence of expression of the naïve markers *KLF4* and *KLF17*, while genes associated with the formative and

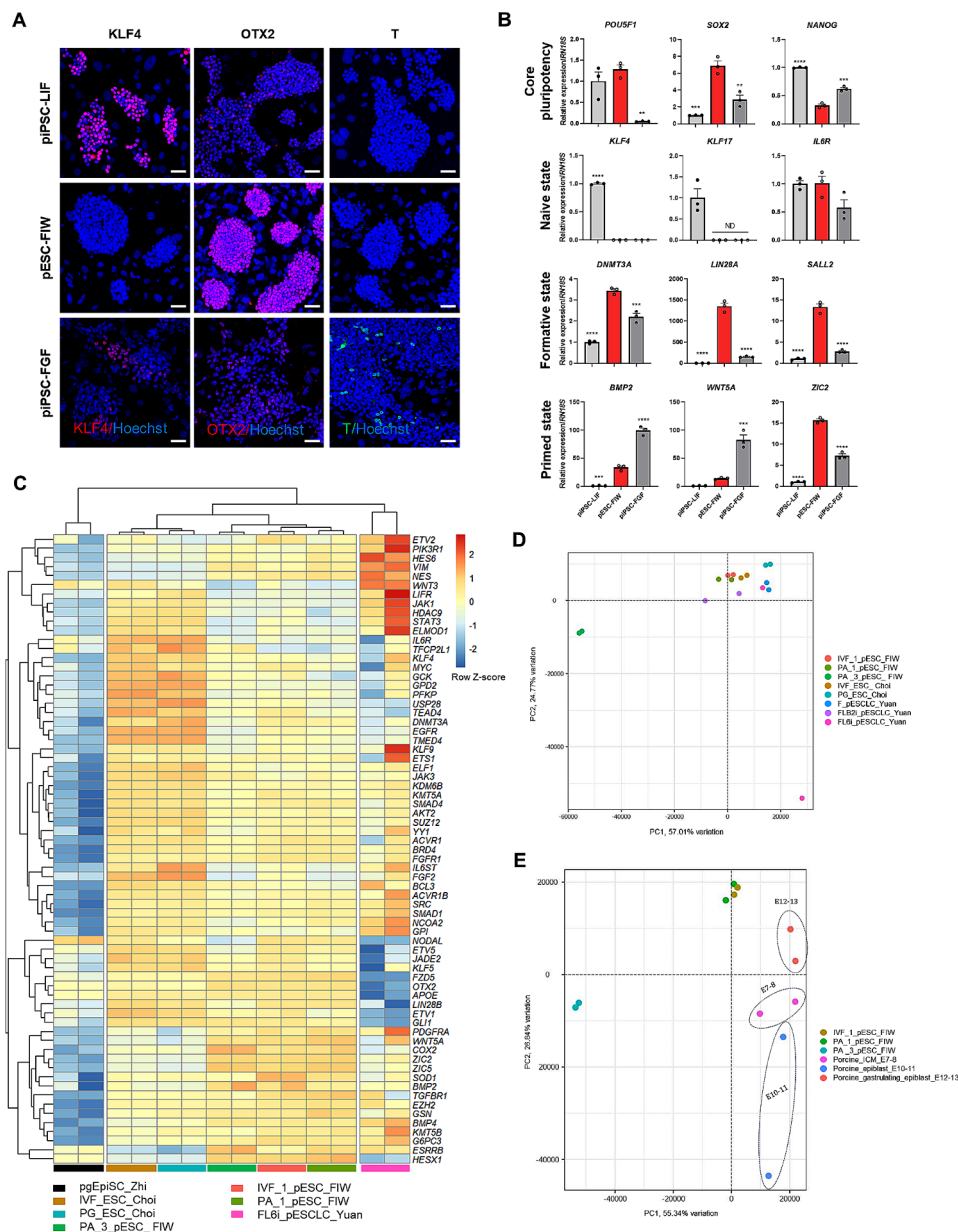


**Fig. 4** Comparative gene expression analysis of three pESC-FIW lines and other pluripotent stem cells (PSCs). **A** Immunostaining results of naïve (*KLF4*), formative (*OTX2*), and primed marker (*T*) in piPSC-LIF, pESC-FIW (PA\_3), and piPSC-FGF. Hoechst was used to stain nuclei. Scale bar, 50  $\mu$ m. **B** Quantification of mRNA expression of representative pluripotency marker genes involved in core pluripotency (*POU5F1*, *SOX2*, and *NANOG*), naive state (*KLF4*, *KLF17*, and *IL6R*), formative state (*DNMT3A*, *LIN28A*, and *SALL2*), and primed state (*BMP2*, *WNT5A*, and *ZIC2*). **C** Expression changes of porcine pluripotency genes in the three pESC-FIW lines and reported pESCs. The blue-to-red gradient on the right side of the heatmap indicates low to high gene expression. **D** PCA based on RNA-seq data for three pESC-FIW lines and reported samples of pESCs. **E** PCA based on RNA-seq data from three pESC-FIW lines and three embryonic developmental stage samples. For all graphs, the value represents the mean  $\pm$  SEM. Asterisks indicate statistical significance (\*\*  $p < 0.01$ , \*\*\*  $p < 0.001$ , \*\*\*\*  $p < 0.0001$ ).

primed states were expressed together with core pluripotency markers (Fig. 4B). These results show that the established pESC-FIW has characteristics closer to the primed state than to the naive state. To examine the cellular identity of pESC-FIW, we prepared RNA-seq libraries in duplicates from two PA-ESC lines (PA\_1\_pESC\_FIW and PA\_3\_pESC\_FIW) and one IVF-ESC line (IVF\_1\_pESC\_FIW). First, we performed a comparative transcriptome analysis of the bulk RNA-seq data from pESC-FIW and other pESC lines from previous studies [20, 21, 23]. Heat map analysis of 69 genes related to pig epiblast development [24] showed that pESC-FIW has features more similar to pESC\_Choi [20] than FL6i\_pESC-CLC\_Yuan [21] and in vivo embryo-derived pESC (pgEpiSCs) [24] have gene expression patterns distinct from those of in vitro embryo-derived pESC (Fig. 4C). Principal components analysis (PCA) revealed similarities with pESCs derived from the complex media formulations (Fig. 4D). We further compared the transcriptome with three embryonic developmental stages of pig embryos [32], and the PCA plots grouped pESC-FIW with E12–13 pig embryos (Fig. 4E). Taken together, these results suggest that pESC-FIW exhibits features of gastrulating epiblast cells and has primed pluripotency.

#### Adaptation of self-renewal and pluripotency in feeder-free conditions

We maintained pESC-FIW in the same culture medium in various matrices (Matrigel, Fibronectin, Laminin-521 (LN521), and VTN-N) to confirm that they could adapt to feeder-free conditions. Although the characteristics of EMT processes, such as nuclear localization of CTNBN1 or the expression of EOMES, were not observed (Figure S1D, E), a significant decrease in the transcript levels of the pluripotency markers *POU5F1* and *NANOG* (Additional file 1: Figure S1A) and upregulation of genes related to EMT (Additional file 1: Figure S1B), and gastrulation (Additional file 1: Figure S1C) were confirmed under feeder-free conditions. These observations indicate that without a feeder layer, using three factors in the culture condition cannot completely maintain the pluripotency of pESC-FIW.

To improve the feeder-free environment, we modified the FIW culture conditions by adding small molecules. First, we supplemented the cells with Activin A (Act A), an important member of the TGF $\beta$  superfamily and is known as a growth factor that supports the expansion of human ESCs under feeder-free conditions [33]. In our study, there was no difference in AP activity between the groups (Fig. 5A). The addition of Act A increased the proportion of POU5F1-positive cells (Fig. 5B); however, ultimately, lower transcript levels of *POU5F1* and *NANOG* were observed than those observed under the feeder condition (Fig. 5C). The second factor added to improve

culture conditions is TGF $\beta$ 1, which pathway interacts with master transcription factors regulating human ESC (hESC) status and differentiation [34]. Consistent with Act A, TGF  $\beta$ 1 supplementation showed similar AP activity (Fig. 5D) and insufficient expression of pluripotency markers compared to levels under feeder conditions (Fig. 5E, F). These results suggest that although the TGF $\beta$ /Smad pathway is essential for maintaining the pluripotency of pESC-FIW, additional pathways are required to preserve pluripotency as much as feeder condition.

We investigated feeder-free adaptation using the commercial medium mTeSR that contains TGF $\beta$ 1. The pESC-FIW cultured in mTeSR showed a denser morphology than those grown under FIW conditions, and uniform AP activity was observed (Figure S2A). Gene expression analysis revealed similar expression levels of *POU5F1*, *SOX2*, and *NANOG* in the feeder and mTeSR conditions (Additional file 1: Figure S2B). These results were confirmed at the protein level using immunostaining. Under FIW conditions, pESC-FIW showed partial expression of POU5F1 and NANOG (Additional file 1: Figure S2C). In contrast, all three transcription factors showed homogeneous expression under the mTeSR condition (Additional file 1: Figure S2D).

Next, we conducted several tests using four matrices to determine whether there was an extracellular matrix that could replace Matrigel, which varied from batch to batch and contained an unknown animal component. We cultured pESC-FIW in the mTeSR medium containing various extracellular matrices for at least three passages and assessed the efficiency of cell attachment, survival, and proliferation. Fibronectin showed a higher cell attachment efficiency than Matrigel, and LN521 and VTN-N showed similar results to Matrigel (Fig. 6A). Cell survival and proliferation were similar in all four matrices, including Matrigel (Fig. 6B, C). We examined the AP activities (Fig. 6D) of pESC cultured in each matrix and confirmed that the transcript levels of core pluripotency markers were similar to those of feeder conditions (Fig. 6E). On the contrary, immunostaining results showed the heterogeneous expression of POU5F1 in pESCs maintained under the LN521 condition (Additional file 1: Figure S3A), unlike in those under the fibronectin (Fig. 6I) and VTN-N conditions (Additional file 1: Figure S3B).

We selected fibronectin as an alternative to Matrigel for further analysis. Cell survival (24 h) and proliferation (72 h) were measured in the presence or absence of the ROCK inhibitor Y-27632. Treatment with the ROCK inhibitor for 24 h was essential for single-cell survival and proliferation of feeder-free pESC (Fig. 6F, G). With respect to the dissociation reagent, TrypLE was the most efficient solution compared to Accutase, Trypsin, and Versene (Fig. 6H). Immunostaining of pESCs in the fibronectin condition showed homogeneous expression of

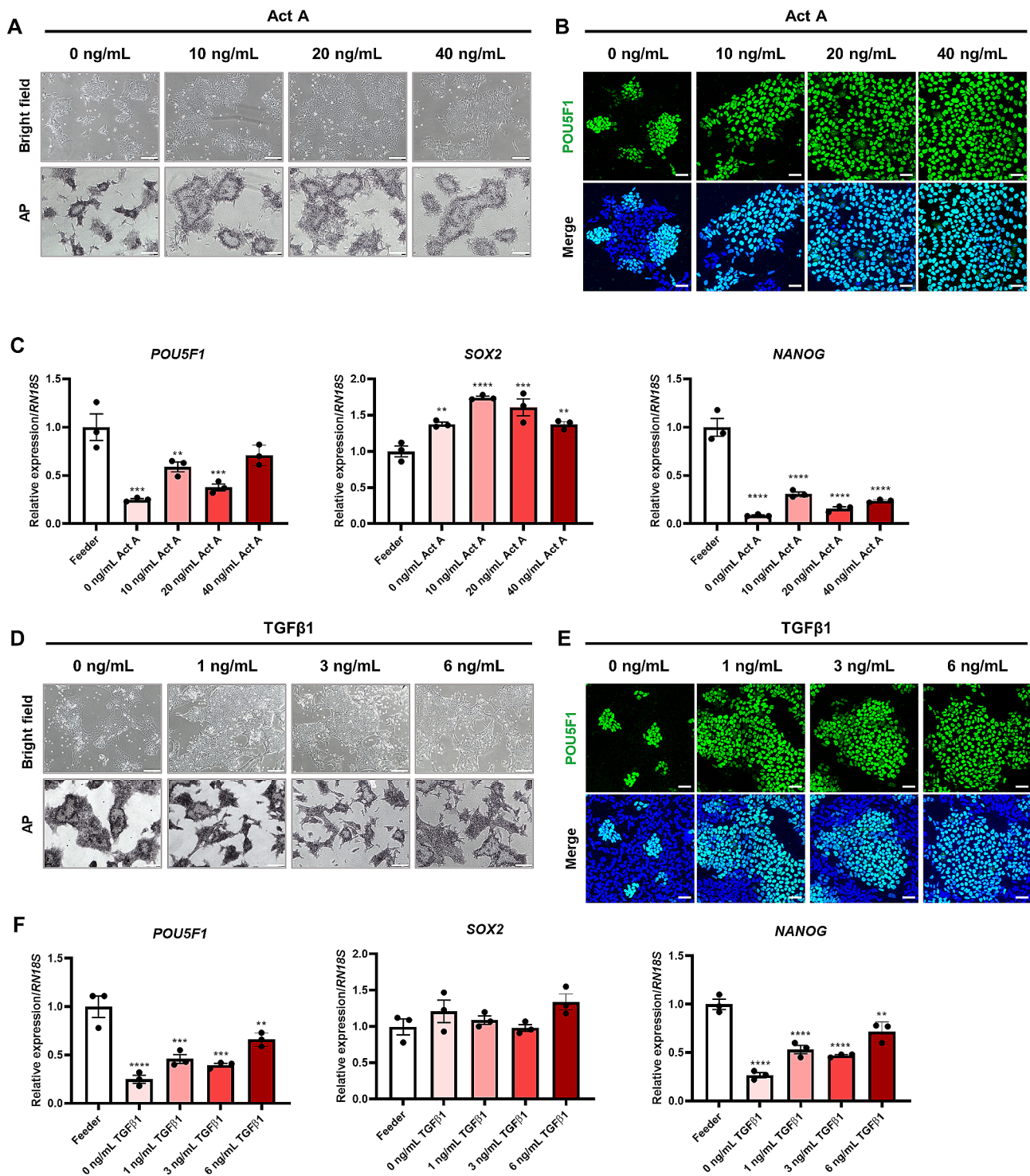


**Fig. 5** Characteristics of pESC-FIW grown under Matrigel with modified culture media. **A** Comparison of morphology and AP staining in pESC-FIW cultured with various concentrations of activin A (Act A). Scale bar, 200  $\mu$ m. **B** Immunostaining for the pluripotency marker POU5F1. The nucleus is indicated by Hoechst. Scale bar, 50  $\mu$ m. **C** Quantification of mRNA expression of representative pluripotent marker genes *POU5F1*, *SOX2*, and *NANOG*. **D** Comparison of morphology and AP staining in pESC-FIW cultured with various concentrations of TGF $\beta$ 1. Scale bar, 200  $\mu$ m. **E** Quantification of mRNA expression of representative pluripotent marker genes *POU5F1*, *SOX2*, and *NANOG*. **F** Immunostaining for the pluripotency marker POU5F1. The nucleus is indicated by Hoechst. Scale bar, 50  $\mu$ m. For all graphs, the value represents the mean  $\pm$  SEM. Asterisks indicate statistical significance (\* $p$  < 0.05, \*\* $p$  < 0.01, \*\*\* $p$  < 0.001, \*\*\*\* $p$  < 0.0001). Cell line PA\_3\_pESC\_FIW were used.

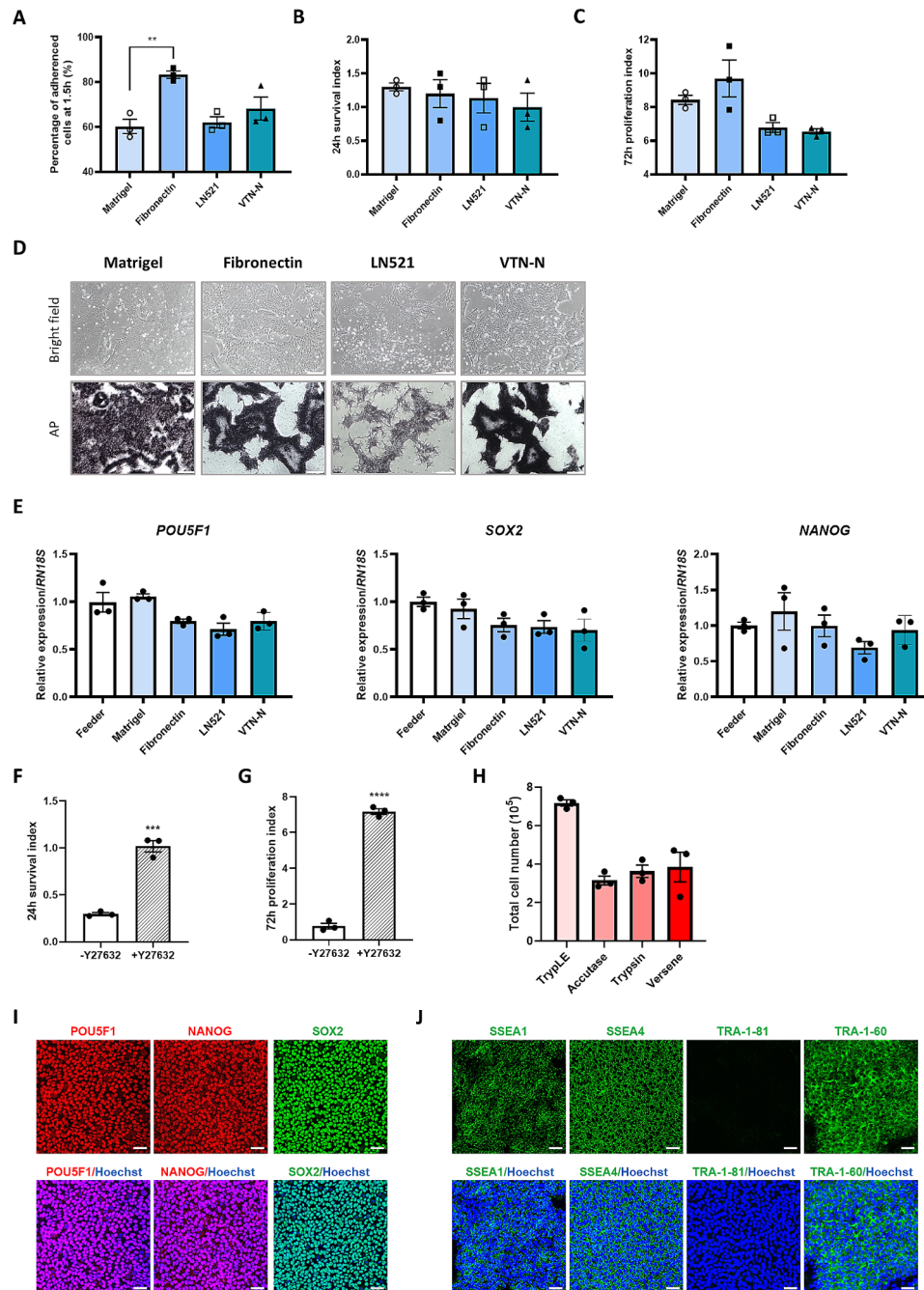


**Fig. 6** Analysis of the effects of different matrix proteins on feeder-free cultured pESC. **A** The percentages of adherent pESC at 1.5 h after seeding. **B** Survival of dissociated pESCs 24 h after seeding. **C** Proliferation of pESC at 72 h after seeding. For **B**, **C**, the index represents the cell number at a specific time point divided by the number of seeding cells. For **A–C**,  $n = 3$  biologically independent samples. PA-pESC were used. **D** Representative morphologies (top) and AP activity (bottom) of feeder-free pESC with different extracellular matrix. Scale bar, 200  $\mu\text{m}$ . **E** Quantification of mRNA expression of core pluripotency marker genes by qRT-PCR in pESC under various matrix conditions. **F**, **G** Survival and proliferation of feeder-free pESC cells under Rock-inhibitor treatment. PA\_3\_pESC\_FIW was used. The index represents the cell number at a specific time point divided by the number of seeding cells.  $n = 3$  biologically independent samples. **H** Dissociation of feeder-free pESC cells using different dissociation reagents. Cell numbers are calculated after dissociation. **I** and **J** Immunostaining of the pluripotency markers POU5F1, NANOG, and SOX2 (**I**) and pluripotency surface markers SSEA1, SSEA4, TRA-1-81, and TRA-1-60 (**J**) in pESC cultured under the fibronectin condition. Hoechst was used to stain nuclei. Scale bar, 50  $\mu\text{m}$ . For all graphs, the value represents the mean  $\pm$  SEM. Asterisks indicate statistical significance (\*\*  $p < 0.01$ , \*\*\*  $p < 0.001$ , \*\*\*\*  $p < 0.0001$ ). Cell line PA\_3\_pESC\_FIW were used.

POU5F1, SOX2, NANOG, SSEA1, SSEA4, and TRA-1-60, but not TRA-1-81, as in the feeder-condition (Fig. 6I, J). The differentiation ability was confirmed by assessing EB formation (Additional file 1: Figure S3C). Taken together, these results demonstrated that the established pESC-FIW can adapt to feeder-free conditions in mTeSR media.

## Discussion

In this study, we attempted to develop a new simplified serum-free medium supporting pluripotency and self-renewal of pig PSCs from in vitro-derived embryos. We performed blastocyst seeding on the feeder layer using different basal media, namely DMEM/F10, DMEM/F12, and  $\alpha$ -MEM, which are commonly used in pig PSC cultures [11, 12, 14–16, 23, 24], and no colonies were observed under the  $\alpha$ -MEM condition. The  $\alpha$ -MEM medium lacks six inorganic salts, including cupric sulfate, ferric nitrate, magnesium chloride, and zinc sulfate, which are present in the other two media. Several reports have demonstrated the relevance of inorganic salts to stem cell migration and pluripotency [35–3738]. It is assumed that these factors create an environment for migration and pluripotency of pig inner cell mass.

We used a combination of the small molecules FGF2, IWR-1, and CHIR to derive pESC-like colonies, and SOX2-positive cells were observed even when only FGF2 and IWR-1 were added to the medium. In humans and pigs, pluripotency is sustained through the FGF/ERK pathway [39–41], and the proliferation and maintenance of pig epiblasts from E7 to E10 require the presence of FGF2 [24]. IWR-1 is an inhibitor of the canonical WNT pathway that promotes the pluripotency of mouse epiblast stem cells (mEpiSCs) and human ESCs by stabilizing the  $\beta$ -catenin disruption complex in the cytoplasm [42, 43]. The GSK3 $\beta$  inhibitor CHIR99021 (CHIR) balances IWR-1 function and coordinates maintenance of the self-renewal of mouse and human PSCs and also contributes to the proliferation of pig PSCs [24, 43]. This inhibitor has effects on both maintenance of pluripotency and differentiation of mouse, human, and pig PSCs depending on its concentration, and the optimal range for maintenance of pig PSCs was 0.5–1.0  $\mu$ M [24, 43]. However, we observed differentiated cells within early passages, although 0.5  $\mu$ M CHIR was added to the culture medium. In pig embryo development, epiblast-to-ectoderm transition occurs through Wnt/ $\beta$ -catenin signaling from E10 [24]. It seems that GSK3 $\beta$  inhibition induced the differentiation of pig PSCs into the ectodermal lineage in our simplified culture condition. For this reason, we established pig PSCs using FGF2 and IWR-1, but insufficient growth was confirmed compared to that of other pig PSCs. To improve self-renewal capacity, we derived a new PSC line, called pESC-FIW, by adding the

SRC inhibitor WH-4-023, which blocks the EMT process and maintains self-renewal of naïve human stem cells and pgEpiSCs [24, 31, 44], observing a short doubling time and improved single cell clonal efficiency. This PSC line expressed pluripotency markers with a dome-shape morphology and was capable of stable long-term culture through single-cell passage. The absence of any one of the three factors affected the pluripotency and self-renewal of pESC-FIW.

Pig pluripotency can be divided into three states (naïve, formative, and primed) according to epiblast development [24]. The naïve state is classified as E4–E6, and hub genes in the JAK/STAT3 signaling pathway are highly expressed. The formative state is classified as E7–E10, where Act A and FGF2 receptors are highly expressed. The primed state is classified as E11–E14, and catenin signaling activity during this stage is significantly increased. We assessed the pluripotency features of pESC-FIW by comparing with those of other pig PSCs. We confirmed the absence of KLF4 expression, which indicates a naïve pluripotent state [45, 46], by immunostaining and qRT-PCR data, and comparative transcriptome analysis showed high similarity to pig ESC\_Choi [20] and E12–13 gastrulating epiblasts [32]. The pig ESC\_Choi has the same culture conditions as pESC-FIW, including FGF2 and IWR-1, and showed primed pluripotency characteristics with flattened morphology. Although pESC-FIW has a dome-shape morphology and single cell passage ability as represented by naïve PSCs [47], its pluripotency is closer to the primed state.

Feeder-free adaptation was performed to increase the utilization of PSCs, but the FIW culture medium did not support pluripotency under four matrices type, even though Act A or TGF $\beta$ 1 was added. Act A is a growth factor that supports the pluripotency of hESCs and human iPSCs (hiPSCs) in feeder-independent cultures [33, 48]. Act A controls the expression of NANOG, which prevents neuroectodermal differentiation [49]. The Activin and TGF $\beta$  pathways share the downstream effectors Smad2 and Smad3 [50]. These pathways are considered to have similar functions, although only Act A allowed feeder-free adaptation in bovine ESCs [51]. In our study, a pluripotency similar to that under the feeder condition was maintained when switching to mTeSR medium, suggesting that TGF $\beta$ , insulin, transferrin, cholesterol, lipids, pipercolic acid, and GABA components, which were not included in FIW medium, support pluripotency.

Here, we successfully developed a simplified serum-free medium containing FGF2, IWR-1, and WH-4-023 through basal medium and small molecule tests and established a new pig PSC line, pESC-FIW. These cells support single-cell passage, express pluripotency markers, and differentiate into three germ layers in vitro and in vivo. They also showed capacity for stable long-term

culture, with a consistent dome-shape morphology, high proliferation ability, and normal karyotype. We validated the feeder-free expansion of pESC-FIW utilizing the mTeSR medium. The culture medium we developed in this study can reduce the costs and time spent on maintaining pig PSCs when they are used for research on genetic manipulation, differentiation induction, and further study of cellular behaviors.

## Conclusions

In summary, we developed a simplified serum-free medium by combination of FGF, IWR-1, and WH-4-023 that support pluripotency, single-cell passage, and stable long-term culture with high proliferation potency of pig PSCs. Although it is necessary to confirm whether the pluripotency of piPSCs can be maintained in FIW medium, the easy-to-maintain pESC-FIW can be used for research on porcine species, such as assessing cell fate decisions, and on the cultured meat field.

## Abbreviations

AP	Alkaline phosphatase
BSA	Bovine serum albumin
COC	Cumulus-oocyte complexes
DPBS	Dulbecco's phosphate-buffered saline
DT	Doubling time
EB	Embryoid body
EDSC	Embryonic disk stem cells
ESC	Embryonic stem cells
FBS	Fetal bovine serum
ICM	Inner cell mass
IVF	In vitro fertilization
KSR	KnockOut Serum Replacement
LIF	Leukemia inhibitory factor
MEF	Mouse embryonic fibroblast
PA	Parthenogenetic activation
PCA	Principal components analysis
PEF	Porcine embryonic fibroblasts
PSC	Pluripotent stem cells
SEM	Standard error of the mean
ZP	Zona pellucida

## Supplementary Information

The online version contains supplementary material available at <https://doi.org/10.1186/s13287-024-03858-2>.

Supplementary Material 1

## Acknowledgements

The authors are grateful to Jongpil Kim from Dongguk University for providing the piPSC-LIF cell line. We thank Eun-Jeong Kim for her several technical assistance, including ovarian sampling.

## Author contributions

H.C. and S.-H.H. both contributed to the conceptualization, validation, and writing – original draft preparation. H.C., D.O., M.K., J.L., L.C., A.J., H.Z., E.K., G.L., H.J., and C.M. all contributed to the methodology and formal analysis. S.-H.H. contributed funding acquisition. All authors have read and approved the submitted version of the manuscript.

## Funding

This work was supported, in part, by a grant from the "National Research Foundation of Korea Grant funded by the Korean Government

(2020R1A2C2008276)", "Technology Innovation Program (20023068) funded by the Ministry of Trade, Industry & Energy (MOTIE, Korea)", and "Korea Institute of Planning and Evaluation for Technology in Food, Agriculture, Forestry and Fisheries (IPET) through Agriculture and Food Convergence Technologies Program for Research Manpower development funded by Ministry of Agriculture, Food and Rural Affairs (MAFRA) (grant number: RS-2024-00398561, RS-2024-00399475).

## Data availability

The datasets used or analyzed during the current study are available from the corresponding author upon reasonable request. The accession number for the RNA-seq data of pESC-FIW reported in this paper is GEO GSE240454. For comparative studies, datasets of pig preimplantation embryos, ESC\_Choi, pESCLC\_Yuan, and pgEpiSC\_Zhi, were obtained from the GEO database (GEO: GSE92889, GSE120031, GSE126150, and CRA003960, respectively).

## Declarations

### Ethics approval and consent to participate

This study was conducted in strict accordance with the Guide for the Care and Use of Laboratory Animals from the National Veterinary and Quarantine Services. The study protocol was approved by the Institutional Animal Care and Use Committee at Chungbuk National University on March 15, 2023 under the project name "Development of porcine midbrain organoids by the analysis of midbrain differentiation mechanism using pluripotent stem cells" (Approval Number: CBNUA-2082-23-02) and "Establishment of porcine embryonic stem cells in simplified serum free media and feeder free expansion" (Approval Number: CBNUA-2243-24-01) on April 1, 2024.

### Consent for publication

Not applicable.

### Competing interests

The authors declare that they have no competing interests.

### Author details

<sup>1</sup>Veterinary Medical Center, College of Veterinary Medicine, Laboratory of Veterinary Embryology and Biotechnology (VETEMBIO), Chungbuk National University, 1 Chungdae-ro, Seowon-gu, Cheongju, Republic of Korea

<sup>2</sup>Institute of Stem Cell and Regenerative Medicine (ISCRM), Chungbuk National University, Cheongju, Republic of Korea

<sup>3</sup>Vet-ICT Convergence Education and Research Center (VICERC), Chungbuk National University, Cheongju, Republic of Korea

<sup>4</sup>Chungbuk National University Hospital, Cheongju, Republic of Korea

<sup>5</sup>Department of Companion Animal Industry, Semyung University, Jecheon 27136, Republic of Korea

<sup>6</sup>Laboratory of Molecular Diagnostics and Cell Biology, College of Veterinary Medicine, Gyeongsang National University, Jinju, Republic of Korea

<sup>7</sup>Department of Neurology, Institute for Cell Engineering, School of Medicine, Johns Hopkins Medicine, Baltimore, MD, USA

<sup>8</sup>Department of Veterinary Anatomy and Animal Behavior, College of Veterinary Medicine, BK21 FOUR Program, Chonnam National University, Gwangju, Republic of Korea

Received: 13 December 2023 / Accepted: 23 July 2024

Published online: 07 August 2024

## References

1. Kobayashi T, Zhang H, Tang WWC, Irie N, Withey S, Klisch D, et al. Principles of early human development and germ cell program from conserved model systems. *Nature*. 2017;546:416–20. <https://doi.org/10.1038/nature22812>. PubMed:28607482.
2. Masaki H, Nakauchi H. Interspecies chimeras for human stem cell research. *Development*. 2017;144:2544–7. <https://doi.org/10.1242/dev.151183>. PubMed:28720651.

3. Dar ER, Gugjoo MB, Javaid M, et al. Adipose tissue- and bone marrow-derived mesenchymal stem cells from Sheep: culture characteristics. *Anim (Basel)*. 2021;11(8):2153. <https://doi.org/10.3390/ani11082153>. PubMed:34438611.
4. Singh B, Mal G, Verma V, et al. Stem cell therapies and benefaction of somatic cell nuclear transfer cloning in COVID-19 era. *Stem Cell Res Ther*. 2021;12(1):283. <https://doi.org/10.1186/s13287-021-02334-5>. PubMed:33980321.
5. Niu D, Wei HJ, Lin L, George H, Wang T, Lee IH, et al. Inactivation of porcine endogenous retrovirus in pigs using CRISPR-Cas9. *Science*. 2017;357:1303–7. <https://doi.org/10.1126/science.aan4187>. PubMed:28798043.
6. Yan S, Tu Z, Liu Z, Fan N, Yang H, Yang S, et al. A huntingtin knockin pig model recapitulates features of selective neurodegeneration in Huntington's disease. *Cell*. 2018;173:989–1002. <https://doi.org/10.1016/j.cell.2018.03.005>. e13. e1013.
7. Yue Y, Xu W, Kan Y, Zhao HY, Zhou Y, Song X, et al. Extensive germline genome engineering in pigs. *Nat Biomed Eng*. 2021;5:134–43. <https://doi.org/10.1038/s41551-020-00613-9>. PubMed:32958897.
8. Notarianni E, Laurie S, Moor RM, Evans MJ. Maintenance and differentiation in culture of pluripotential embryonic cell lines from pig blastocysts. *J Reprod Fertil Suppl*. 1990;41:51–6. PubMed:2213715.
9. Chen LR, Shiue YL, Bertolini L, Medrano JF, BonDurant RH, Anderson GB. Establishment of pluripotent cell lines from porcine preimplantation embryos. *Theriogenology*. 1999;52:195–212. [https://doi.org/10.1016/S0093-691X\(99\)00122-3](https://doi.org/10.1016/S0093-691X(99)00122-3). PubMed:10734388.
10. Li M, Zhang D, Hou Y, Jiao L, Zheng X, Wang WH. Isolation and culture of embryonic stem cells from porcine blastocysts. *Mol Reprod Dev*. 2003;65(4):429–34. <https://doi.org/10.1002/mrd.10301>. PubMed:12840816.
11. Cha HJ, Yun Ji, Han NR, Kim HY, Baek S, Lee SH, et al. Generation of embryonic stem-like cells from in vivo-derived porcine blastocysts at a low concentration of basic fibroblast growth factor. *Reprod Domest Anim*. 2018;53:176–85. <https://doi.org/10.1111/rda.13088>. PubMed:29110378.
12. Hou DR, Jin Y, Nie XW, Zhang ML, Ta N, Zhao LH, et al. Derivation of porcine embryonic stem-like cells from in vitro-produced blastocyst-stage embryos. *Sci Rep*. 2016;6:25838. <https://doi.org/10.1038/srep25838>. PubMed:27173828.
13. Park JK, Kim HS, Uh KJ, Choi KH, Kim HM, Lee T, et al. Primed pluripotent cell lines derived from various embryonic origins and somatic cells in pig. *PLoS ONE*. 2013;8:e52481. <https://doi.org/10.1371/journal.pone.0052481>. PubMed:23326334.
14. Siriboon C, Lin YH, Kere M, Chen CD, Chen LR, Chen CH, et al. Putative porcine embryonic stem cell lines derived from aggregated four-celled cloned embryos produced by oocyte bisection cloning. *PLoS ONE*. 2015;10:e0118165. <https://doi.org/10.1371/journal.pone.0118165>. PubMed:25680105.
15. Vassiliev I, Vassilieva S, Beebe LF, Harrison SJ, McIlfratrick SM, Nottle MB. In vitro and in vivo characterization of putative porcine embryonic stem cells. *Cell Reprogramming*. 2010;12:223–30. <https://doi.org/10.1089/cell.2009.0053>. PubMed:20677936.
16. Xue B, Li Y, He Y, Wei R, Sun R, Yin Z, et al. Porcine pluripotent stem cells derived from IVF embryos contribute to chimeric development in vivo. *PLoS ONE*. 2016;11:e0151737. <https://doi.org/10.1371/journal.pone.0151737>. PubMed:26991423.
17. Gao X, Nowak-Imialek M, Chen X, Chen D, Herrmann D, Ruan D, et al. Establishment of porcine and human expanded potential stem cells. *Nat Cell Biol*. 2019;21(6):687–99. <https://doi.org/10.1038/s41556-019-0333-2>. PubMed:31160711.
18. Ramos-Ibeas P, Sang F, Zhu Q, et al. Pluripotency and X chromosome dynamics revealed in pig pre-gastrulating embryos by single cell analysis. *Nat Commun*. 2019;10(1):500. <https://doi.org/10.1038/s41467-019-08387-8>. PubMed:30700715.
19. Zhang X, Xue B, Li Y, et al. A novel chemically defined serum- and feeder-free medium for undifferentiated growth of porcine pluripotent stem cells. *J Cell Physiol*. 2019;234(9):15380–94. <https://doi.org/10.1002/jcp.28185>. PubMed:30701540.
20. Choi KH, Lee DK, Kim SW, Woo SH, Kim DY, Lee CK. Chemically defined media can maintain pig pluripotency network in vitro. *Stem Cell Rep*. 2019;13:221–34. <https://doi.org/10.1016/j.stemcr.2019.05.028>. PubMed:31257130.
21. Yuan Y, Park J, Tian Y, Choi J, Pasquariello R, Alexenko AP, et al. A six-inhibitor culture medium for improving naïve-type pluripotency of porcine pluripotent stem cells. *Cell Death Discov*. 2019;5:104. <https://doi.org/10.1038/s41420-019-0184-4>. PubMed:31240131.
22. Li Y, Wu S, Li X, Guo S, Cai Z, Yin Z, et al. Wnt signaling associated small molecules improve the viability of pPSCs in a PI3K/Akt pathway dependent way. *J Cell Physiol*. 2020;235:5811–22. <https://doi.org/10.1002/jcp.29514>. PubMed:32003013.
23. Kinoshita M, Kobayashi T, Planells B, Klisch D, Spindlow D, Masaki H, et al. Pluripotent stem cells related to embryonic disc exhibit common self-renewal requirements in diverse livestock species. *Development*. 2021;148:d199901. <https://doi.org/10.1242/dev.199901>. PubMed:34874452.
24. Zhi M, Zhang J, Tang Q, Yu D, Gao S, Gao D, et al. Generation and characterization of stable pig pregastrulation epiblast stem cell lines. *Cell Res*. 2022;32:383–400. <https://doi.org/10.1038/s41422-021-00592-9>. PubMed:34848870.
25. Abeydeera LR, Day BN. In vitro penetration of pig oocytes in a modified tris-buffered medium: effect of BSA, caffeine and calcium. *Theriogenology*. 1997;48:537–44. [https://doi.org/10.1016/s0093-691x\(97\)00270-7](https://doi.org/10.1016/s0093-691x(97)00270-7). PubMed:16728149.
26. Choi IY, Lim H, Huynh A, Schofield J, Cho HJ, Lee H, et al. Novel culture system via wirelessly controllable optical stimulation of the FGF signaling pathway for human and pig pluripotency. *Biomaterials*. 2021;269:120222. <https://doi.org/10.1016/j.biomaterials.2020.120222>. PubMed:32736809.
27. Martin M. Cutadapt removes adapter sequences from high-throughput sequencing reads. *EMBnet J*. 2011;17(1):10. <https://doi.org/10.14806/ej.17.1.200>. PubMed:28715235.
28. Dobin A, Davis CA, Schlesinger F, et al. STAR: ultrafast universal RNA-seq aligner. *Bioinformatics*. 2013;29(1):15–21. <https://doi.org/10.1093/bioinformatics/bts635>. PubMed:23104886.
29. Li B, Dewey CN. RSEM: accurate transcript quantification from RNA-Seq data with or without a reference genome. *BMC Bioinformatics*. 2011;12:323. <https://doi.org/10.1186/1471-2105-12-323>. PubMed:21816040.
30. Liu S, Bou G, Sun R, et al. Sox2 is the faithful marker for pluripotency in pig: evidence from embryonic studies. *Dev Dyn*. 2015;244(4):619–27. <https://doi.org/10.1002/dvdy.24248>. PubMed:25619399.
31. Lee J, Park YJ, Jung H. Protein kinases and their inhibitors in pluripotent stem cell fate regulation. *Stem Cells Int*. 2019;2019:1569740. <https://doi.org/10.1155/2019/1569740>. PubMed:3142815.
32. Secher JO, Ceylan A, Mazzoni G, Mashayekhi K, Li T, Muenthaissong S, et al. Systematic in vitro and in vivo characterization of leukemia-inhibiting factor- and fibroblast growth factor-derived porcine induced pluripotent stem cells. *Mol Reprod Dev*. 2017;84:229–45. <https://doi.org/10.1002/mrd.22771>. PubMed:28044390.
33. Beattie GM, Lopez AD, Bucay N, Hinton A, Firpo MT, King CC, et al. Activin A maintains pluripotency of human embryonic stem cells in the absence of feeder layers. *Stem Cells*. 2005;23:489–95. <https://doi.org/10.1634/stemcells.2004-0279>. PubMed:15790770.
34. Mullen AC, Wrana JL. TGF-beta family signaling in embryonic and somatic stem-cell renewal and differentiation. *Cold Spring Harb Perspect Biol*. 2017;9. <https://doi.org/10.1101/cshperspect.a022186>. PubMed:28108485.
35. Fathi E, Farahzadi R. Zinc Sulphate mediates the stimulation of cell proliferation of rat adipose tissue-derived mesenchymal stem cells under high intensity of EMF exposure. *Biol Trace Elem Res*. 2018;184(2):529–35. <https://doi.org/10.1007/s12011-017-1199-4>. PubMed:29189996.
36. Díaz-Tocados JM, Herencia C, Martínez-Moreno JM, et al. Magnesium chloride promotes Osteogenesis through Notch signaling activation and expansion of mesenchymal stem cells. *Sci Rep*. 2017;7(1):7839. <https://doi.org/10.1038/s41598-017-08379-y>. PubMed:28798480.
37. He X, Zhu Y, Yang L, et al. MgFe-LDH nanoparticles: a promising leukemia inhibitory factor replacement for Self-Renewal and Pluripotency Maintenance in cultured mouse embryonic stem cells. *Adv Sci (Weinh)*. 2021;8(9):2003535. <https://doi.org/10.1002/advs.202003535>. PubMed:33977050.
38. Celauro E, Mukaj A, Fierro-González JC, Wittung-Stafshede P. Copper chaperone ATOX1 regulates pluripotency factor OCT4 in preimplantation mouse embryos. *Biochem Biophys Res Commun*. 2017;491(1):147–53. <https://doi.org/10.1016/j.bbrc.2017.07.064>. PubMed:28711491.
39. Choi KH, Lee DK, Oh JN, Son HY, Lee CK. FGF2 Signaling plays an important role in maintaining pluripotent state of Pig Embryonic Germ cells. *Cell Reprogram*. 2018;20(5):301–11. <https://doi.org/10.1089/cell.2018.0019>. PubMed:30204498.
40. Xu C, Inokuma MS, Denham J, et al. Feeder-free growth of undifferentiated human embryonic stem cells. *Nat Biotechnol*. 2001;19(10):971–4. <https://doi.org/10.1038/nbt1001-971>. PubMed:11581665.
41. Zhao H, Jin Y. Signaling networks in the control of pluripotency [published correction appears in *Curr Opin Genet Dev*. 2020;61:91]. *Curr Opin Genet Dev*. 2017;46:141–8. <https://doi.org/10.1016/j.cde.2017.07.013>. PubMed:28806594.



42. Martins-Neves SR, Paiva-Oliveira DI, Fontes-Ribeiro C, Bovée JVMG, Cleton-Jansen AM, Gomes CMF. IWR-1, a tankyrase inhibitor, attenuates Wnt/beta-catenin signaling in cancer stem-like cells and inhibits in vivo the growth of a subcutaneous human osteosarcoma xenograft. *Cancer Lett.* 2018;414:1–15. <https://doi.org/10.1016/j.canlet.2017.11.004>. PubMed:29126913.
43. Kim H, Wu J, Ye S, Tai CI, Zhou X, Yan H, et al. Modulation of beta-catenin function maintains mouse epiblast stem cell and human embryonic stem cell self-renewal. *Nat Commun.* 2013;4:2403. <https://doi.org/10.1038/ncomms3403>. PubMed:23985566.
44. Collier AJ, Rugg-Gunn PJ. *BioEssays.* 2018;40(5):e1700239. <https://doi.org/10.1002/bies.201700239>. PubMed:29574793. Identifying Human Naïve Pluripotent Stem Cells - Evaluating State-Specific Reporter Lines and Cell-Surface Markers.
45. Dunn SJ, Martello G, Yordanov B, Emmott S, Smith AG. Defining an essential transcription factor program for naive pluripotency. *Science.* 2014;344(6188):1156–60. <https://doi.org/10.1126/science.1248882>. PubMed:24904165.
46. Martello G, Bertone P, Smith A. Identification of the missing pluripotency mediator downstream of leukaemia inhibitory factor. *EMBO J.* 2013;32(19):2561–74. <https://doi.org/10.1038/emboj.2013.177>. PubMed:23942233.
47. Ying QL, Wray J, Nichols J, et al. The ground state of embryonic stem cell self-renewal. *Nature.* 2008;453(7194):519–23. <https://doi.org/10.1038/nature06968>. PubMed:18497825.
48. Tomizawa M, Shinozaki F, Sugiyama T, Yamamoto S, Sueishi M, Yoshida T. Activin A is essential for feeder-free culture of human induced pluripotent stem cells. *J Cell Biochem.* 2013;114:584–8. <https://doi.org/10.1002/jcb.24395>. PubMed:22991093.
49. Vallier L, Mendjan S, Brown S, Chng Z, Teo A, Smithers LE, et al. Activin/Nodal signalling maintains pluripotency by controlling nanog expression. *Development.* 2009;136:1339–49. <https://doi.org/10.1242/dev.033951>. PubMed:19279133.
50. Pauklin S, Vallier L. Activin/Nodal signalling in stem cells. *Development.* 2015;142:607–19. <https://doi.org/10.1242/dev.091769>. PubMed:25670788.
51. Soto DA, Navarro M, Zheng C, Halstead MM, Zhou C, Guiltinan C, et al. Simplification of culture conditions and feeder-free expansion of bovine embryonic stem cells. *Sci Rep.* 2021;11:11045. <https://doi.org/10.1038/s41598-021-90422-0>. PubMed:34040070.

### Publisher's Note

Springer Nature remains neutral with regard to jurisdictional claims in published maps and institutional affiliations.